Journal Pre-proofs

Novel skin permeation enhancers based on amino acid ester ionic liquid: Design and permeation mechanism

Luyao Zheng, Zhiyuan Zhao, Ye Yang, Yaming Li, Chengxiao Wang

PII: S0378-5173(20)30013-2
DOI: https://doi.org/10.1016/j.ijpharm.2020.119031
Reference: IJP 119031

To appear in: *International Journal of Pharmaceutics*

Received Date: 6 September 2019
Revised Date: 15 December 2019
Accepted Date: 10 January 2020

Please cite this article as: L. Zheng, Z. Zhao, Y. Yang, Y. Li, C. Wang, Novel skin permeation enhancers based on amino acid ester ionic liquid: Design and permeation mechanism, *International Journal of Pharmaceutics* (2020), doi: https://doi.org/10.1016/j.ijpharm.2020.119031

Novel skin permeation enhancers based on amino acid ester ionic liquid: Design and permeation mechanism

Luyao Zheng▲, Zhiyuan Zhao▲, Ye Yang, Yaming Li*, Chengxiao Wang*

School of Life Science and Technology, Kunming University of Science and Technology, Kunming, 650500, China

*Corresponding author: Chengxiao Wang, wcx1192002@126.com

Yaming Li, liym@kmust.edu.cn

▲: The authors contributed equally to the work.

ABSTRACT

This study developed novel ionic liquids (ILs) based on amino acids. We first screened 15 methyl amino acid ester hydrochlorides ([AAC1]Cl) for their skin permeation enhancements using 5-Fluorouracil (5-Fu) and Hydrocortisone (HC) as model drugs. Glycine methyl ester hydrochloride ([GlyC1]Cl), L-proline methyl ester hydrochloride ([L-ProC1]Cl), and L-leucine methyl ester hydrochloride ([L-LeuC1]Cl) were selected, and their ester sites were modified with different carbon chains (C8 and C12). The resulting ILs showed improved permeation to the two drugs. TEWL and CLSM assays revealed the moderation effects of the modified ILs on skin barrier function, whereas L-proline dodecyl ester hydrochloride ([ProC12]Cl) and L-leucine dodecyl ester hydrochloride ([L-LeuC12]Cl) exhibited the strongest activities. Permeation mechanisms were further investigated by ATR-FTIR, solid-NMR, SEM, and TEM analyses. The results suggested that [L-ProC12]Cl and [L-LeuC12]Cl combined the advantages of amino acid esters and IL solvent and could interact with the intercellular lipid domain by the multi-functions of lipid fluidization and lipid extraction, which were observed in a dosage- and time-dependent manner. Additionally, pathological examination suggested that the amino acid ester-based ILs (AAE-ILs) had good biocompatibility. In conclusion, this study has generated novel chemical penetration enhancers (CPEs) based on AAE-ILs and may be potentially utilized in drug transdermal delivery systems (TDDSs).

KEYWORDS: Ionic liquid; Amino acid ester; Penetration enhancers; Transdermal drug delivery; Skin permeability

1 Introduction

Chemical penetration enhancer (CPE) is an essential element of drug transdermal delivery systems (TDDSs) because these can accelerate drug penetration through the skin without causing serious irritation and damage (Prausnitz and Langer, 2008; Wang et al., 2018). Commonly used CPEs include sulfoxide, azone, fatty acids, aliphatic

alcohols, and terpenoids (Chen et al., 2014). In recent years, a series of compounds such as terpenoids (Chen et al., 2016), glycosides (Kopecna et al., 2017), menthol ester derivatives (Chen et al., 2013; Zhao et al., 2008), polypeptides (Kumar et al., 2015), amino acid derivatives (Janůšová et al., 2013; Novotny et al., 2011), and carvone ester derivatives (Wang et al., 2013) have been proven to enhance drug percutaneous absorption. However, despite these findings, only a few products are clinically used due to irritation and other safety issues that have not yet been clarified (Marwah et al., 2016). Therefore, the exploration of chemicals to safely improve skin permeability remains an extensive research area.

Ionic liquids, which are composed of a large and asymmetric organic cation and an anion, have favorable features such as non-volatility, recyclability, and inherent tenability (Das and Roy, 2013; Zhang et al., 2006). Most importantly, ILs are designer solvents that can be synthesized with specific chemical and physical properties by changing the anion/cation combination or introducing specific functional groups (Das and Roy, 2013). Therefore, ILs can hopefully replace highly volatile organic solvents across a wide range of applications, including clean energy, electrochemistry, and separation science.

In the last decades, ILs have been investigated in terms of pharmaceutical applications (Egorova and Ananikov, 2018; Egorova et al., 2017; Tanner et al., 2018) and of particular importance is its utilization in transdermal drug delivery (Sidat et al., 2019; Zakrewsky et al., 2014). Numerous studies have revealed that imidazolium ILs can significantly increase drug solubility, which in turn enhance systematic stability and establishes a high concentration gradient for skin permeation (Caparica et al., 2018; Jaitely et al., 2008; Mizuuchi et al., 2008; Moniruzzaman et al., 2010b; Tanner et al., 2018). Then they have been used as ingredients into microemulsions for TDDSs (Goindi et al., 2014; Moniruzzaman et al., 2010a; Moniruzzaman et al., 2010c; Monti et al., 2017). On the other hand, transformation of the active pharmaceutical ingredient (API) into ILs formluation were emerged as an effective approach to improve the skin permeability due to the moderation of the thermodynamic activity (Halayqa et al., 2017;

Moshikur et al., 2018).

ILs were aslo reported as chemical permeation enhancers (CPEs)(Kubota et al., 2016; Santos de Almeida et al., 2017; Sidat et al., 2019). In particular, choline and geranic acid (CAGE) based ILs can signiciantly improve transdermal delivery of macromolecule such as insulin and dextran(Qi and Mitragotri, 2019; Tanner et al., 2018; Wu et al., 2019). We previously assessed the permeation promotion profiles of imidazolium ILs, and elucidated their mechanisms using a quantitative structure-activity relationship (QSAR) model (Zhang et al., 2017). Furthermore, 1-hydroxyethyl-3-methylimidazolium chloride ([HOEIM]Cl) and 1-butyl-3-methylimidazolium dodecanesulfate ([BMIM]$C_{12}SO_3$) were screened as the aqueous phase and surfactant phases of microemulsions to assist percutaneous absorption of dencichine (Wang et al., 2018).

Although ILs showed great potential in CPEs, these have been proven to be resistant to biodegradation and inducing skin irritations (Moniruzzaman et al., 2010c; Wang et al., 2018). Further applications were limited by some toxicological, ecological, as well as economic issues. Use of biodegradable components for the preparation of ILs is a promising approach to overcome these drawbacks (Chen et al., 2008; Fukaya et al., 2007; Tao et al., 2006). Successful procedures have been reported, which include lactates, sugars, and amino acids (Fukaya et al., 2007). Among these, amino acid-based ILs are highly valued due to their simple synthetic precursors and chiral centers with specific physical/chemical properties (Caparica et al., 2018; Chen et al., 2008; Fukumoto et al., 2005; Tao et al., 2005). It is worth noting that amino acid derivatives have been demonstrated their capacity for skin permeation enhancement and thus have been used as CPEs in previous studies (Janůšová et al., 2013; Novotny et al., 2011). By combining the properties of amino acids and ILs together, one can infer that amino acid-based ILs might be designed and developed as novel CPEs. However, investigations related to the development of novel CPEs using amino acid-based ILs are limited.

Here, we report the amino acid ester-based ILs (AAE-ILs) as CPEs using molecular

design strategies. A variety of methyl amino acid ester hydrochlorides ([AAC1]Cl) have been screened for their *in vitro* skin permeation enhancement using hydrocortisone (HC) and 5-Fluorouracil (5-Fu) as model drugs. Among these, three [AAC1]Cls were selected, and the ester groups were modified with different carbon chains (C8 and C12) to enhance skin permeability. Furthermore, the permeation mechanism of these novel CPEs was deeply investigated. Our work demonstrated the significant skin permeation promotion profiles of [AAE]Cl, which are of great potential in TDDS and would facilitate further development and utilization of ILs in pharmaceutical industries.

2 Methods and Materials

2.1 Chemicals

The 15 species of ILs, namely, L-leucine methyl ester hydrochloride ([L-LeuC1]Cl), L-proline methyl ester hydrochloride ([L-ProC1]Cl), L-alanine methyl ester hydrochloride ([L-AlaC1]Cl), L-phenylalanine methyl ester hydrochloride ([L-PheC1]Cl), L-methionine methyl ester hydrochloride ([L-MetC1]Cl), L-isoleucine methyl ester hydrochloride ([L-IleC1]Cl), L-hydroxyproline methyl ester hydrochloride ([L-HypC1]Cl), glycine methyl ester hydrochloride ([GlyC1]Cl), L-histidine methyl ester dihydrochloride ([L-HisC1]Cl), L-valine methyl ester hydrochloride ([L-ValC1]Cl), L-arginine methyl ester dihydrochloride ([L-ArgC1]Cl), L-glutamic acid dimethyl ester hydrochloride ([L-GluC1]Cl), L-threonine methyl ester hydrochloride ([L-ThrC1]Cl), L-tryptophane methyl ester hydrochloride ([L-TrpC1]Cl), and L-serine methyl ester hydrochloride ([L-SerC1]Cl), were directly purchased from Aladdin Industrial Corporation, with purity of 99%. Trypsin (damas-beta), 5-fluorouracil, hydrocortisone, glycine, L-leucine, L-proline, and 1-dodecanol were purchased from Aladdin Industrial Corporation. *p*-Toluene sulfonic acid (99.5%) was purchased from DaMao Chemical Reagent Factory. 1-Octanol was provided by Chron Chemicals. Deuterated chloroform was purchased from Cambridge Isotope Laboratories, Inc. Nile Red (98%) and fluorescein sodium (90%) were provided by Shanghai Yuanye Bio-Technology Co., Ltd. 5-Fu (≥99%, lot number: F596000) and HC (≥98%, lot number: DC14224000) were purchased from Aladdin industrial

Corporation. Laurocapram (Azone®, CAS:59227-89-3, damas-beta, ≥98%), Diethylene Glycol Monoethyl Ether (Transcutol®, CAS:111-90-0, ≥98%) and Tween 20 (AR CAS:9005-64-5, 98%) were purchased from ShaoYuan Chemical Reagent Factory. All the other chemicals were of analytical grade and used without further purification.

2.2 Animals

The Wistar rats (240-280 g) and Kunming mice (18-22 g) used in this study were supplied by the Experimental Animal Center of Kunming Medical University (License number: SCXK 2014-007), Kunming, China. The animals were housed at ambient standard temperature, with a 12-h day/night cycle, and fed a standard pellet diet and water. The protocol of the experiments was approved by the Experimental Animal Welfare and Ethics Committee of Kunming University of Science and Technology. All efforts were made to minimize animal suffering and to limit the number of animals used.

2.3 *In vitro* drug percutaneous absorptions

2.3.1 Skin preparation

The dorsal skin of Kunming mice was used for *in vitro* skin experiment. After sacrificing the mice, their subcutaneous fats and sub-dermal tissues were carefully removed from the dorsal skin with scissors and cleaned with saline solution. The skin samples were then cut into appropriate sizes and stored at -20°C until further use (used within two weeks of preparation).

2.3.2 Sample preparation

HC and 5-Fu were used as model drugs. Different [AAE]Cls, serving as CPEs, were added into normal saline in advance and adjusted to a concentration of 1% and 5% separately. After that, HC and 5-Fu were accurately weighed and dissolved in the prepared solution at a concentration of 1 and 5 mg/mL, respectively. Then, the drug solution was ultrasonically treated for 10 min for *in vitro* percutaneous absorption assays. Three Commercial CPEs, namely Azone, Tween 20 and Transcutol® were used as controls.

2.3.3 Franz diffusion experiment

The *in vitro* skin permeation experiment was conducted in a Franz diffusion cell (YB-P6, Tianguang Instrument Co., Ltd. Tianjin, China) with a diffusion area of 1.33 cm^2 and receptor volume of 15.0 mL. The prepared skin was mounted between the donor and receptor cell by the dermis side in contact with the receiver compartment. Then, 2.0 mL of test sample and 15.0 mL of PBS (pH = 7.4) were added into the donor cell and receptor cell, respectively. During the experiment, the receptor solution was stirred at 350 rpm and a temperature of 37 ± 1°C. At predetermined intervals (0, 1, 2, 4, 6, 8, 10, and 12 h), 2.0 mL of the sample was collected from the receptor cells and immediately replaced by an equal volume of fresh medium. The sink condition was maintained during the entire experimental process. The collected samples were directly subjected to HPLC analysis to determine the drug content. Three skin permeation parameters, J (steady permeation flux), $Q_{12\,h}$ (drug-permeated amount at 12 h), and ER (enhancement ratio) were calculated according to our previous study (Zhang et al., 2017).

2.3.4 HPLC analysis

The drug content was analyzed by an HPLC system consisting of SPD-20A variable-wavelength ultraviolet absorbance detector, an LC-20AB pump, and an SIL-20A automatic sampler (Shimadzu Corporation, Tokyo, Japan) and packed with YMC-PACK ODS-AM C18 column (250×4.6 mm, 5 μm). The HPLC methods of the two drugs were established as described elsewhere, with some modifications (Chen et al., 2013; Sintov et al., 2009), and detailed in the supporting information (Fig. S1, Fig. S2, table S1 and table S2).

2.4 Synthesis and characterization of [AAE]-derivative IL

The ester groups of the selected [AAE]Cl were modified with different carbon chains (C8 and C12) to enhance skin permeability. Six [AAE]Cls, namely, L-glycine octyl ester hydrochloride ([GlyC8]Cl), L-glycine dodecyl ester hydrochloride ([GlyC12]Cl), L-leucine octyl ester hydrochloride ([LeuC8]Cl), L-leucine dodecyl ester hydrochloride

([LeuC12]Cl), L-proline octyl ester hydrochloride ([ProC8]Cl), and L-proline dodecyl ester hydrochloride ([ProC12]Cl) were synthesized as previously described (Joondan et al., 2017; Nichol et al., 2013) with modifications, and the general synthesis procedure is shown in Fig. 1. The detailed information of the synthesis method can be found in the supporting information.

Characterization of the synthesized products was performed using a 600-MHz spectrometer (Bruker Avance III HD 600, Bruker BioSpin, Switzerland). The ^{1}H-NMR and ^{13}C-NMR spectrum as well as the data are listed in Fig. S3 (Joondan et al., 2017; Nichol et al., 2013; Vávrová et al., 2003b). the FTIR spectrum of the products are listed in Fig. S4.

2.5 Skin permeability assay

2.5.1 In vivo TEWL assay

For transepidermal water loss (TEWL) measurements, 28 rats were equally divided into seven groups consisting of blank (treated with normal saline) and six [AAE]Cl-treated groups. Approximately 24 h prior to application, the dorsal skin of the animals was carefully shaved. Then, 1 h before administration, the TEWL values of the shaved sites were measured in advance using a Vapometer evaporimeter (Delfin, Kuopio, Finland). Approximately 0.1 mL of the test solution (prepared as described in Section 2.3.2 without adding the drug) was then applied on the shaved site every 15 min. After 1 h, the test sites were carefully washed and dried. Then, the TEWL values at 0.5 1, 2, 4, and 6 h were determined. The enhancement ratio (ER) of permeation was calculated by the proportion of TEWL value of test groups to the blank group at the same time interval (Wang et al., 2018).

2.5.2 In vitro CLSM assay

In vitro confocal laser scanning microscopy (CLSM) assays were performed using Franz diffusion cells as described in Section 2.3.3. Rhodamine B and sodium fluorescein were chosen as fluorophores. The test solution was prepared by adding the two fluorophores into the [AAE]Cl solutions (prepared in Section 2.3.2) to a

concentration of 1%. At the beginning of the experiments, 0.1 mL of the test sample and 15.0 mL of PBS (pH = 7.4) were added into the donor cell and receptor cell, respectively. After 1 h, the rat skin sample was recovered, washed, and directly examined in terms of fluorescent intensities (CLSM 410 inverted confocal microscope, Nikon A1, Jena, Germany).

2.6 Mechanisms of action

2.6.1 Animal treatment

Two selected [AAE]Cls were employed as CPEs to investigate their effects on the barrier function of skin at different concentration levels (1% and 5%) and exposure times (1 and 4 h). Wistar rats were used as model animals. Untreated rats were used as negative controls, and those treated with normal saline were used as positive controls.

The dorsal skin of the animals was carefully shaved in advance. Then, 0.1 mL of the test solution was then applied onto the shaved site every 30 min until the end of the experiment, except for the negative control group. The residual solution was then washed with normal saline and dried at room temperature for 30 min. After that, the animals were sacrificed, and epidermal samples were prepared following the methods described in Section 2.3.1 and used in various evaluations.

2.6.2 ATR-FITR assay

The epidermal samples from different groups were directly subjected to ATR-FTIR evaluation (Thermo Fisher Scientific, Nicolet iS 10, USA). ZnSe was used as the internal reflection crystal, with an incident angle of 45°. The stratum corneum was placed faced down onto the crystal, and the spectrum was recorded between 4,000 and 400 cm^{-1}.

2.6.3 Solid-NMR assay

The stratum corneum (SC) was separated from the epidermis, as previously described (Narishetty and Panchagnula, 2004; Pham et al., 2016). Briefly, full-thickness skin was placed on a Petri dish and soaked in PBS solution with 0.2% trypsin at 37°C overnight.

The sheets of SC were removed from the tissue using forceps, washed, dried, and further ground into powder.

NMR experiments were performed at ^{13}C resonance frequencies of 125 MHz on a Bruker Avance AVII-500 NMR spectrometer equipped with a Bruker Efree 4 mm MAS (magic angle spinning) probe (for the first batch) or a 4 mm CP/MAS HX probe (for the second batch) and at a spinning frequency of 5 kHz.

2.6.4 SEM assay

The epidermis samples were immersed in 10% buffered formalin. After fixation, the samples were dehydrated using an ethanol gradient (30–100%, v/v) and dried in a critical point dryer (Quorum, K850). The blocks were coated with gold using an ion sputtering instrument (IXRF, MSP-2S) and then visualized under an SEM (Hitachi, SU8100) (de Graaff et al., 2003; Manconi et al., 2011).

2.6.5 TEM assay

The epidermis samples were fixed in 1% osmic acid for 2 h (20°C). After fixation, the tissue sections were washed with PBS and dehydrated using an ethanol gradient (70–100%). Then, the specimens were infiltrated in two different ratios of epoxy resin and acetone (1:1, 1:2, v/v) and finally changed for pure resin overnight. The tissue cubes were then embedded in resin in polyethylene capsules for 12 h at 37°C and 48 h at 60°C. Then, the samples were sectioned at the thickness of 60–80 nm using an ultramicrotome (Leica UC7). After negative staining using uranyl acetate and lead citrate, the specimens were observed using a TEM (Hitachi, HT7700) (Yang et al., 2016).

2.7 Histopathological and toxic examination

2.7.1 skin irritation

The skin samples prepared in Section 2.6.1 were fixed with 10% buffered formalin. After fixation, the samples were dehydrated in an ethanol gradient (30–100%, v/v) and then stained with hematoxylin and eosin. Finally, the specimens were observed under

a high-powered light microscope (DM13000 M, Wetzlar, Germany).

2.7.2 Cytotoxicity

The toxicities of [L-ProC12]Cl and [L-LeuC12]Cl were evaluated on HaCaT spontaneously immortalized human keratinocytes and 3T3 Swiss albino mouse embryonic fibroblasts. The cell lines were cultivated as described in our previous work (Wang et al., 2018). Cell viability was determined using a 3-(4,5-dimethylthiazol-2-yl)-2,5-diphenyltetrazolium bromide (MTT) uptake assay after 48 h incubation with ILs at different concentration. The TC_{50} value, i.e., the enhancer concentration that caused a 50% decrease in cell viability after 48 h incubation were then calculated.

2.8. Statistical analyses

All statistical analyses were conducted using SPSS 19.0 (SPSS, Inc., USA), and the values were expressed as the mean ± standard deviation. The results were deemed statistically significant at $p<0.05$ and <0.01.

3 Results

3.1 Screening for [AAE]Cls

In this study, fifteen [AAE]Cls consisting of different amino acids were first screened by an *in vitro* transdermal delivery assay of 5-Fu and HC, as shown in Fig. 2 and Table 1. The [AAE]Cls exerted different influences on drug transdermal delivery. For 5-Fu, [L-ValC1]C1, [L-TrpC1]Cl, and [L-MetC1]Cl imparted negative effects on drug permeation, whereas the other 12 [AAE]CL showed positive effects. Among these, [L-LeuC1]Cl, [GlyC1]Cl, [L-ProC1]Cl, and [L-ThrC1]Cl provided relatively higher enhancement ($p<0.01$, relative to the other [AAE]Cls). In contrast, only [L-PheC1]Cl, [L-ProC1]Cl, [GlyC1]Cl, [L-LeuC1]Cl, and [L-ArgC1]Cl showed enhanced HC permeation, whereas the other 10 [AAE]Cls retarded drug permeation. Interestingly, [L-LeuC1]Cl, [GlyC1]Cl, and [L-ProC1]Cl were the three ILs that have the stronger enhancements than the others ($p<0.01$, compared to the other [AAE]Cls) but were comparable to 5-Fu. Furthermore, the three [AAE]Cls also showed better performances

than the conventional CPEs such as Azone®, Tween 20 and Transcutol®. Therefore, we inferred that the L-Pro, L-Leu, and Gly esters might be the key structures for skin permeation and could be designed as novel CPEs in their IL form.

3.2 Design and characterization of novel [AAE]Cls

Six [AAE]Cls, namely, [L-LeuC8]Cl, [L-LeuC12]Cl, [GlyC8]Cl, [GlyC12]Cl, [L-ProC8]Cl, and [L-ProC12]Cl were successfully synthesized using the corresponding amino acids by esterification and acidification reactions (Fig. 1). The products were characterized by NMR and FTIR, as shown in Fig. S3 and S4. Furthermore, the physical state, yields and purities of ILs were listed in table S2.

After modification, the six [AAE]Cls were examined in terms of skin permeation enhancement (Fig. 3 and Table 2). For 5-Fu, the modified ILs significantly increased the Q_{12h}, Flux, and P_m, as compared with their original structure ($p<0.01$). Furthermore, better penetration was observed when the alkyl chain was lengthened from C8 to C12, whereas [L-LeuC12]Cl showed the highest ER value of 7.14, which was 2.60- and 1.66-fold that of [L-LeuC1]Cl ($p<0.01$) and [L-LeuC8], respectively. However, the contributions of these [AAE]Cls on HC permeation were found to be less significant, while the modified Pro derivatives showed better activities than the Leu and Gly derivatives. In addition, there were no statistical differences between the C8 and C12 groups.

3.3 Effects of various [AAE]Cls on skin permeability

3.3.1 TEWL evaluation

TEWL is widely accepted as the key parameter that is related to skin hydration because the considerable TEWL values indicated disturbances involving skin barrier properties (Zhang et al., 2017). Fig. 4a-c shows that the skin applications of the six [AAE]Cls significantly increase the TEWL values. At the initial time, the ER ranged from 1.8 to 3.4 at 1 h after administration, and the highest was observed in the [L-LeuC12]Cl group, which coincided with the drug permeation results. After removal of the test solution,

the TEWL values stayed at high levels for 1 h and then gradually decreased. At the end of the experiment (6 h after removal of the solution), the TEWL of each test group reverted to the normal levels, which showed no statistical differences with the negative control. Meanwhile, the ER values decreased to about 1 (Fig. 4d), suggesting the attenuation of the promotional effects. Therefore, the results indicated that the six [AAE]Cls can effectively moderate the skin barrier functions in a reversible manner with no permanent skin damage.

3.3.2 CLSM evaluation

Since [L-LeuC12]Cl and [L-ProC12]Cl exhibited remarkable effects on both drug delivery and TEWL evaluation, the two ILs were selected for CLSM examination. Fig. 5 shows that the blank group (received 1% fluorescent-normal saline) offered relatively low fluorescence intensity as well as permeation depth (up to 20 μm for sodium fluorescein and 60 μm for Rhodamine B) in mice skin. In contrast, the two ILs significantly increased both the penetration depth and intensity in a dose-dependent manner, and Leu-based ILs showed better skin penetration. Under the treatment of 5% [L-LeuC12]Cl, higher fluorescence intensities could be detected through the test depth.

3.4 Mechanisms of action

3.4.1 ATR-FTIR evaluation

The ATR-FTIR is a powerful tool that has been used to elucidate the molecular organization of the lipid matrix in the SC. In the present study, [L-LeuC12]Cl and [L-ProC12]Cl were employed to assess their influences on SC. For the control sample, the characteristic absorption peaks of the lipid were at 2,846.27 (C-H symmetric vibration), 2,915.52 (C-H asymmetric vibration), and 1,738.60 cm^{-1} (C=O vibration). The characteristic absorption peaks of the keratin were at 1,646.42 and 1,542.50 cm^{-1} (NH-C=O vibration), as shown in table 3.

The two ILs were found to produce some shifts in the absorption peaks in a dose-dependent manner (Fig. 6 and table 3). After administration of 1% IL for 4 h, no statistical differences between the blank and test groups were observed. However, when

the concentration was increased to 5%, significant shifts were observed at 2,921.32, 2,852.21, 1,641.60, and 1,536.69 cm^{-1} ($p<0.05$) in [L-ProC12]Cl group and 2922.01, 2853.48 ($p<0.01$), 1641.60, and 1,537.61 cm^{-1} ($p<0.05$) in the [L-LeuC12]Cl groups, suggesting changes in the configuration of both lipid and keratin induced by the two ILs. Furthermore, the influences were also observed to be time-dependent. At the administration time of 1 h, no statistical differences were observed between the test groups and the blank. When treatment time was prolonged to 4 h, significant shifts were observed in the characteristic peaks of lipid as well as keratin (table 3).

3.4.2 Solid-NMR evaluation

Solid-NMR was also employed to investigate the effect of the two ILs on the structure of SC molecular segments. The majority of the lipid acyl chain $(CH2)_n$ resonates within a range of 30-34 ppm, in which the all-*trans* conformation (AT) is visualized at ~34 ppm, and the liquid-like distribution of trans/gauche conformation (TG) is assigned at ~31 ppm (Björklund et al., 2013; Earl and VanderHart, 1979; Nowacka et al., 2010; Pham et al., 2016). Fig. 7 shows that strong AT signals were observed at ~34 ppm, but the TG signals were relatively weak, suggesting the presence of solid lipid domains in the SC. However, when the ILs were applied, TG signals can be detected at ~31 ppm, and the TG/AT proportion was elevated.

3.4.3 SEM evaluation

As compared to Fig. 8a and Fig. 8e, introduction of two ILs brought clear differences to the skin microstructures. After co-incubation with 5% [L-ProC12]CL for 1 h, the keratin particles in the corneocytes were less densely arranged. The surface of the horny layers was swollen, indicating an increase in total thickness and distinct gaps between the lamellae of the multilayer SC lipids (Fig. 8b). When the incubation time was increased to 4 h, the differences were even more significant (Fig. 8d). The compact and dense SC lipids became loose and fluidized. The lamellae of the multilayer were stripped from the epidermis and separated from each other, indicating that the lipid extraction effects were in a time-dependent manner. Additionally, the effects were

found to be dose-dependent. The microstructural variations in the skin sample subjected to 5% [L-ProC12]Cl treatments (Fig. 8d) were more pronounced compared to that treating with 1% ILs (Fig. 8c). Similar phenomena were observed in the [L-LeuC12]Cl groups (Figs.8 f-h). The results of SEM indicated that lipid extraction might be another route for the ILs to moderate the skin permeability (Manconi et al., 2011; Xie et al., 2017).

3.4.4 TEM evaluation

Lipid extraction effects were also revealed by TEM evaluation. In the blank group, the outer layer of the keratinocyte SC clearly presented the "brick and mortar" ultrastructure (Fig. 9a), which was regularly and closely arranged, overlaid layer-by-layer, and had densely spaced and flat-shaped lipid composition between the layers. Therefore, the SC layer functions in barrier protection and is considered to be the major obstacle to the transdermal absorption of drugs (Yang et al., 2016). When normal saline was applied, no significant differences were observed (Fig. 9e). However, the ultrastructure of the epidermis in the two ILs groups exhibited relative differences. Taking [L-ProC12]Cl for example, after co-incubation with the IL solution for 1 h, the SC multilayer increased in thickness. The "brick structure" became loose, and the gap increased and showed irregular arrangement and lower degree of overlaying (Fig. 9b). When the incubation time was increased to 4 h, lipid extractions were observed. The lamellae of the multilayer were stripped from the epidermis and separated from each other (Fig. 9d), which coincided with the SEM results. Furthermore, the effects were also found to be time-dependent, as shown in Fig. 9c and d.

3.5 Safety examination

Skin irritation potential of the [AAE]Cl solution was assessed by preliminary histopathological evaluation and shown in Fig. 10. No histopathological findings were observed in both the epidermal and the dermal layers of the skin biopsies in the blank group. After administration of [L-ProC12]C1 and [L-LeuC12]Cl at different times and concentration levels, there were no obvious edema and tissue necrosis, as well as

inflammatory cell infiltration, which implied a good biocompatibility between the CPEs and skin, indicating no skin irritations were induced after transdermal administration of [AAE]Cl formulation. Furthermore, In the cytotoxicity assay, both the two [AAE]Cls showed negligible toxicities towards HaCaT and 3T3 cells (Fig. 11). The TC_{50} of [L-ProC12]Cl in 3T3 and HaCaT cell were 325 μM and 352 μM respectively, Notably, the[L-LeuC12]Cl toxicities strongly depended on the cell type: the TC_{50} of in 3T3 cells was 387 μM, which was much higher than that of the HaCaT cells (177 μM).

Discussion

Excised human skin from surgery is the best available model for skin absorption (Wertz, 1996). However, in view of the difficulties associated with human skin, animal skin is routinely used as a substitute. Though there are distinct differences between animal skin and human skin with regarded to the permeability, the porcine skin has gained wide acceptance as a representative model for human skin (Haigh and Smith, 1994)**. Due to the limitation of experimental conditions, the only way we can get porcine ear skin is to purchase it from the local meat market. However, it was hard for us to obtain such a large skin (about 800cm^2) from one porcine ear. If using the porcine ear skin separately, the gender, age and feeding conditions of the animals cannot be unified, and the individual differences would be large enough to invalidate the experimental results. By contrast, Kunming mouse, an outbreed strain of laboratory animal, has been widely utilized in related skin permeation studies as well as regulatory toxicity and sensitivity studies throughout China (Ashara and Shah, 2016). They are readily available, small, cheap and easy for sampling data. In our current work, Kunming mice from the same batch were used. That means the genetic stability and other parameters of the animals can be well controlled and unified. Meanwhile, the parallel experiments can be easily realized to minimize the individual differences. Therefore, the data repeatability and stability can be guaranteed.**

5-fluorouracil (5-Fu) was a water-soluble BCS class III drug (LogP=-0.89, Mw=

130.08)(Fang et al., 2004). Meanwhile. Hydrocortisone (HC) is a hydrophobic corticosteroid (LogP=1.61, Mw=362.46)(El-Kattan et al., 2000). Due to the molecular properties of the two drugs, both of them were widely employed as model drugs to estimate the activities of various penetration enhancers and vehicles (El-Kattan et al., 2000; Song et al., 2001; Venuganti and Perumal, 2008).

In the ILs screen experiment, we found that the fifteen [AAE]Cl exerted different effects on the in vitro skin permeation of the two model drug. The action of a CPE can be discussed in terms of drug diffusivity and partition coefficient in three pathways i.e., the lipoidal intercellular pathway, the polar transcellular pathway and the transfollicular pathway. As a hydrophilic drug, the permeation of 5-Fu is probably taking place through the transcellular pathway. As indicated by the P*m* (Table 2), the ILs significantly improved the partitioning of the drug into the lipid layers of SC, which is the major challenge of its skin penetration(Kumar et al., 2012). By contrast, the hydrophobic compound HC, favors the lipoidal intercellular pathway rather than the polar transcellular pathway. Moreover, it was noteworthy that the transfollicular pathway accounted for 46% of total penetration flux (Frum et al., 2007; Frum et al., 2008). Therefore, the ILs exerted the partially influences on the skin permeation of HC, which resulted an insignificant effect as compared to that of 5-Fu. Moreover, it was interesting to find that the conventional CPEs showed similar effects with certain [AAE]Cls, such as [L-HypC1]Cl, [L-AlaC1]Cl and [L-PheC1]Cl.

[L-LeuC1]Cl, [GlyC1]Cl, and [L-ProC1]Cl were selected due to their stronger enhancements to the two model drugs. It was reported that substituents at ester site with alkyl chain or other functional groups would increase the permeation activities. In contrast, enhancers with bulkier substituents on nitrogen, showed less effects(Janůšová et al., 2013). In our previous study, we revealed that the effects of imidazolium ILs were found to be directly related to their molecular structure, particularly the alkyl chain length (Wang et al., 2018; Zhang et al., 2017). Therefore, in the current study, the selected [AAE]Cls were modified with different alkyl chains (C8 and C12) at the ester group to enhance their activities.

As suggested by the *in vitro* drug penetration and skin permeability assays, the modified CPEs might improve drug penetration by regulating skin barrier function. After modification, the six [AAE]Cls showed improved permeation activities in relation to alkyl length. The dodecyl ester derivatives provided better performance than their octyl ester analogs. It has been proposed that CPEs with a certain chain length, i.e., around 12 carbons, possess an optimal balance between partition coefficient and affinity to skin (Vávrová et al., 2003a; Vávrová et al., 2003b). Shorter chain fatty acids would have insufficient lipophilicity for skin permeation; when the carbon chain length exceeds 12 or more, the strong affinity made the CPEs closely integrate with SC, rather than pass through it, and that will hamper the contact of drug with SC, resulting in the reduction of skin penetration.

AAE have been demonstrated to be a promising class of CPEs, with a hydrophobic "tail" attached to an amino acid "head" via a biodegradable linkage of ester bond. It was suggested that these amphiphilic compounds could insert directly between the hydrophobic tails of lipid acyl chains and disrupt the packing of lipids, thereby increasing the fluidization of lipids (Kumar et al., 2015). This hypothesis has been further proved in our work. As indicated by the ATR-FTIR spectrum, under the treatment of [AAE]Cls, the lateral packing of the SC lipids transforms from an orthorhombic conformation to a liquid-crystalline manner and the conformation of keratin changed from the α-helix arrangement to the random coil structure, which leads to a loose accumulation of SC proteins with more extensive carbon movement (Boncheva et al., 2008; Schwarz et al., 2013). In Solid-NMR examination, the TG/AT proportion of the SC was elevated. Briefly, a solid crystalline phase or gel phase has a high fraction of AT conformation, whereas the TG is a sign of disordered acyl chains in the liquid crystalline or isotropic liquid phases. Therefore, the increasing of TG/AT proportion suggested an increase in the lipid mobility of the acyl chain and a higher fluidity of SC.

Moreover, when the AAE transformed into the IL formulation, new chemicophysical properties were achieved. SEM and TEM assays suggested a lipid extraction effects of

the [AAE]Cls. The ILs might act as a solvent and exert the permeation enhancement by lipid extraction, which was also observed in some solvents such as DMSO and ethanol (Babita et al., 2006; Panchagnula et al., 2001). Based on the above findings, the selected [AAE]Cl seemed to interact with the intercellular lipid domain by the multi-functions *via* lipid fluidization and lipid extraction(Qi and Mitragotri, 2019; Tanner et al., 2019).

As indicated by the skin irritation and cytotoxicity assay, the modified [AAE]Cl showed neglectable toxicities. The biodegradable linkage of the ester bond could be hydrolyzed after reaching the dermis which was enzymatically active, thus releasing known nontoxic compounds with much less irritation potential than other kinds of CPEs (Janůšová et al., 2013).

4. Conclusions

This study screened novel [AAE]Cl-based CPEs for skin permeation enhancements using 5-Fu and HC as model drugs. [GlyC1]Cl, [L-ProC1]Cl, and [L-LeuC1]Cl were selected, and their ester sites were modified with different carbon chain (C8 and C12). All the obtained products induced excellent permeation enhancements in the two model drugs. The TEWL and CLSM assays revealed the moderation effects of the modified [AAE]Cls on skin barrier function. Among these, [L-ProC12]Cl and [L-LeuC12]Cl exhibited the strongest activities and were further evaluated for their permeation mechanisms by ATR-FTIR, solid-NMR, and SEM and TEM assays. The results suggested that the novel CPEs combined the advantages of amino acid esters and IL solvent and could interact with the intercellular lipid domain via lipid fluidization and lipid extraction. Additionally, pathological examination suggested good biocompatibility between [AAE]Cl and skin. Therefore, this study has demonstrated the significant skin permeation promotion profiles of [AAE]Cl, which may be potentially utilized in TDDS and would facilitate further development and utilization of ILs in the pharmaceutical industries.

Acknowledgments

The National Natural Science Foundation of China (81760642) supported this study.

We thank LetPub (www.letpub.com) for its linguistic assistance during the preparation of this manuscript.

Figure captions

Figure 1. Synthesis of the six [AAE]Cls. a: [GlyC8]Cl; b: [GlyC12]Cl; c: [L-LeuC8]Cl; d: [L-LeuC12]Cl; e: [L-ProC8]Cl, and f: [L-ProC12]Cl.

Figure 2. *In vitro* skin permeation performances of 5-Fu and HC with appearances of the 15 [AAE]Cls. The concentrations of [AAE]Cl were set at 5%, and drug concentrations were set at 5% and 1% for 5-Fu and HC, respectively (n=4, mean ± SD).

Figure 3. *In vitro* skin permeation performances of 5-Fu and HC with appearances of the six modified [AAE]Cls using the original [AAE]Cl as reference. The [AAE]Cl concentrations were set at 5%, and drug concentrations were set at 5% and 1% for 5-Fu and HC, respectively. a: 5-Fu permeation with Gly-based ILs; b: 5-Fu permeation with L-Leu-based ILs; c: 5-Fu permeation with L-Leu-based ILs; d: HC permeation with Gly-based ILs; e: HC permeation with L-Leu-based ILs; and f: HC permeation with L-Pro-based ILs (n=4, mean ± SD).

Figure 4. TEWL values of rat skins treated with the following: a: Gly-based ILs, b: L-Leu-based ILs, and c: L-Pro-based ILs. d: Enhanced ratio (ER) of the TEWL values. The [AAE]Cl concentrations were set at 5% (n=4, mean ± SD).

Figure 5. CLSM evaluations of rat skins treated with [L-LeuC12]Cl or [L-ProC12]Cl. The administration time was 1 h. a: Sodium fluorescein and b: Rhodamine B

Figure 6. ATR-FTIR spectra of rat skins treated with [L-LeuC12]Cl and [L-ProC12]Cl.

Figure 7. Solid-NMR spectra of rat skins treated with [L-LeuC12]Cl and [L-ProC12]Cl. Green line: blank; red line: 5% [L-ProC12]Cl-4h; blue line: 5%[L-LeuC12]Cl-4h.

Figure 8. SEM evaluation of the microstructure of rat skin treated with [L-LeuC12]Cl or [L-ProC12]Cl.

Figure 9. TEM evaluation of the microstructure of rat skin treated with [L-LeuC12]Cl or [L-ProC12]Cl.

Figure 10. Pathological examination of rat skin treated with [L-LeuC12]Cl or [L-ProC12]Cl.

Figure. 11. The viability of 3T3 and HaCaT cell lines after 48 h of incubation with the selected enhancers [L-ProC12]Cl and [L-LeuC12]Cl (n=3).

References

Ashara, K., Shah, K., 2016. Elementary of animal model for percutaneous and ocular penetration. Asian Pacific Journal of Tropical Disease 6, 1007-1010.

Babita, K., Kumar, V., Rana, V., Jain, S., Tiwary, A., 2006. Babita K, Kumar V, Rana V, Jain S, Tiwary AKThermotropic and spectroscopic behavior of skin: relationship with percutaneous permeation enhancement. Curr Drug Deliv 3:95-113. Current drug delivery 3, 95-113.

Björklund, S., Nowacka, A., Bouwstra, J.A., Sparr, E., Topgaard, D., 2013. Characterization of Stratum Corneum Molecular Dynamics by Natural-Abundance 13C Solid-State NMR. PloS one 8, e61889.

Boncheva, M., Damien, F., Normand, V., 2008. Molecular organization of the lipid matrix in intact Stratum corneum using ATR-FTIR spectroscopy. Biochimica et Biophysica Acta (BBA) - Biomembranes 1778, 1344-1355.

Caparica, R., Julio, A., Baby, A.R., Araujo, M.E.M., Fernandes, A.S., Costa, J.G., Santos de Almeida, T., 2018. Choline-Amino Acid Ionic Liquids as Green Functional Excipients to Enhance Drug Solubility. Pharmaceutics 10.

Chen, J., Jiang, Q.D., Chai, Y.P., Zhang, H., Peng, P., Yang, X.X., 2016. Natural Terpenes as Penetration Enhancers for Transdermal Drug Delivery. Molecules 21.

Chen, X., Li, X., Hu, A., Wang, F., 2008. Advances in chiral ionic liquids derived from natural amino acids. Tetrahedron: Asymmetry 19, 1-14.

Chen, Y., Quan, P., Liu, X., Wang, M., Fang, L., 2014. Novel chemical permeation enhancers for transdermal drug delivery. Asian Journal of Pharmaceutical Sciences 9, 51-64.

Chen, Y., Wang, J., Cun, D., Wang, M., Jiang, J., Xi, H., Cui, H., Xu, Y., Cheng, M., Fang, L.,

2013. Effect of unsaturated menthol analogues on the in vitro penetration of 5-fluorouracil through rat skin. International journal of pharmaceutics 443, 120-127.

Das, R.N., Roy, K., 2013. Advances in QSPR/QSTR models of ionic liquids for the design of greener solvents of the future. Molecular diversity 17, 151-196.

de Graaff, A.M., Li, G.L., van Aelst, A.C., Bouwstra, J.A., 2003. Combined chemical and electrical enhancement modulates stratum corneum structure. Journal of Controlled Release 90, 49-58.

Earl, W.L., VanderHart, D.L., 1979. Observations in Solid Polyethylenes by Carbon-13 Nuclear Magnetic Resonance with Magic Angle Sample Spinning. Macromolecules 12, 762-767.

Egorova, K.S., Ananikov, V.P., 2018. Fundamental importance of ionic interactions in the liquid phase: A review of recent studies of ionic liquids in biomedical and pharmaceutical applications. Journal of Molecular Liquids 272, 271-300.

Egorova, K.S., Gordeev, E.G., Ananikov, V.P., 2017. Biological Activity of Ionic Liquids and Their Application in Pharmaceutics and Medicine. Chem Rev 117, 7132-7189.

El-Kattan, A.F., Asbill, C.S., Michniak, B.B., 2000. The effect of terpene enhancer lipophilicity on the percutaneous permeation of hydrocortisone formulated in HPMC gel systems. International journal of pharmaceutics 198, 179-189.

Fang, J.Y., Hung, C.F., Fang, Y.P., Chan, T.F., 2004. Transdermal iontophoresis of 5-fluorouracil combined with electroporation and laser treatment. International journal of pharmaceutics 270, 241-249.

Frum, Y., Bonner, M.C., Eccleston, G.M., Meidan, V.M., 2007. The influence of drug partition coefficient on follicular penetration: In vitro human skin studies. European Journal of

Pharmaceutical Sciences 30, 280-287.

Frum, Y., Eccleston, G.M., Meidan, V.M., 2008. Factors influencing hydrocortisone permeation into human hair follicles: Use of the skin sandwich system. International journal of pharmaceutics 358, 144-150.

Fukaya, Y., Iizuka, Y., Sekikawa, K., Ohno, H., 2007. Bio ionic liquids: room temperature ionic liquids composed wholly of biomaterials. Green Chemistry 9, 1155.

Fukumoto, K., Yoshizawa, M., Ohno, H., 2005. Room temperature ionic liquids from 20 natural amino acids. Journal of the American Chemical Society 127, 2398-2399.

Goindi, S., Arora, P., Kumar, N., Puri, A., 2014. Development of novel ionic liquid-based microemulsion formulation for dermal delivery of 5-Fluorouracil. AAPS PharmSciTech 15, 810-821.

Haigh, J.M., Smith, E.W., 1994. The selection and use of natural and synthetic membranes for in vitro diffusion experiments. European Journal of Pharmaceutical Sciences 2, 311-330.

Halayqa, M., Zawadzki, M., Domańska, U., Plichta, A., 2017. API-ammonium ionic liquid – Polymer compounds as a potential tool for delivery systems. Journal of Molecular Liquids 248, 972-980.

Jaitely, V., Karatas, A., Florence, A.T., 2008. Water-immiscible room temperature ionic liquids (RTILs) as drug reservoirs for controlled release. International journal of pharmaceutics 354, 168-173.

Janůšová, B., Školová, B., Tükörová, K., Wojnarová, L., Šimůnek, T., Mladěnka, P., Filipský, T., Říha, M., Roh, J., Palát, K., Hrabálek, A., Vávrová, K., 2013. Amino acid derivatives as transdermal permeation enhancers. Journal of Controlled Release 165, 91-100.

Joondan, N., Caumul, P., Jhaumeer-Laulloo, S., 2017. Investigation of the physicochemical and biological properties of proline-based surfactants in single and mixed surfactant systems. J Surfactants Deterg 20, 103-115.

Kopecna, M., Machacek, M., Prchalova, E., Stepanek, P., Drasar, P., Kotora, M., Vavrova, K., 2017. Dodecyl Amino Glucoside Enhances Transdermal and Topical Drug Delivery via Reversible Interaction with Skin Barrier Lipids. Pharmaceutical research 34, 640-653.

Kubota, K., Shibata, A., Yamaguchi, T., 2016. The molecular assembly of the ionic liquid/aliphatic carboxylic acid/aliphatic amine as effective and safety transdermal permeation enhancers. European journal of pharmaceutical sciences : official journal of the European Federation for Pharmaceutical Sciences 86, 75-83.

Kumar, S., Sahdev, P., Perumal, O., Tummala, H., 2012. Identification of a Novel Skin Penetration Enhancement Peptide by Phage Display Peptide Library Screening. Molecular pharmaceutics 9, 1320-1330.

Kumar, S., Zakrewsky, M., Chen, M., Menegatti, S., Muraski, J.A., Mitragotri, S., 2015. Peptides as skin penetration enhancers: mechanisms of action. Journal of controlled release : official journal of the Controlled Release Society 199, 168-178.

Manconi, M., Sinico, C., Caddeo, C., Vila, A.O., Valenti, D., Fadda, A.M., 2011. Penetration enhancer containing vesicles as carriers for dermal delivery of tretinoin. International journal of pharmaceutics 412, 37-46.

Marwah, H., Garg, T., Goyal, A.K., Rath, G., 2016. Permeation enhancer strategies in transdermal drug delivery. Drug delivery 23, 564-578.

Mizuuchi, H., Jaitely, V., Murdan, S., Florence, A.T., 2008. Room temperature ionic liquids and

their mixtures: potential pharmaceutical solvents. European journal of pharmaceutical sciences : official journal of the European Federation for Pharmaceutical Sciences 33, 326-331.

Moniruzzaman, M., Kamiya, N., Goto, M., 2010a. Ionic liquid based microemulsion with pharmaceutically accepted components: Formulation and potential applications. Journal of colloid and interface science 352, 136-142.

Moniruzzaman, M., Tahara, Y., Tamura, M., Kamiya, N., Goto, M., 2010b. Ionic liquid-assisted transdermal delivery of sparingly soluble drugs. Chemical communications 46, 1452-1454.

Moniruzzaman, M., Tamura, M., Tahara, Y., Kamiya, N., Goto, M., 2010c. Ionic liquid-in-oil microemulsion as a potential carrier of sparingly soluble drug: characterization and cytotoxicity evaluation. International journal of pharmaceutics 400, 243-250.

Monti, D., Egiziano, E., Burgalassi, S., Chetoni, P., Chiappe, C., Sanzone, A., Tampucci, S., 2017. Ionic liquids as potential enhancers for transdermal drug delivery. International journal of pharmaceutics 516, 45-51.

Moshikur, R.M., Chowdhury, M.R., Wakabayashi, R., Tahara, Y., Moniruzzaman, M., Goto, M., 2018. Characterization and cytotoxicity evaluation of biocompatible amino acid esters used to convert salicylic acid into ionic liquids. International journal of pharmaceutics 546, 31-38.

Narishetty, S.T., Panchagnula, R., 2004. Transdermal delivery of zidovudine: effect of terpenes and their mechanism of action. Journal of controlled release : official journal of the Controlled Release Society 95, 367-379.

Nichol, J.L., Morozowich, N.L., Allcock, H.R., 2013. Biodegradable alanine and phenylalanine alkyl ester polyphosphazenes as potential ligament and tendon tissue scaffolds. Polym Chem-Uk 4, 600-606.

Novotny, M., Klimentova, J., Janusova, B., Palat, K., Hrabalek, A., Vavrova, K., 2011. Ammonium carbamates as highly active transdermal permeation enhancers with a dual mechanism of action. Journal of controlled release : official journal of the Controlled Release Society 150, 164-170.

Nowacka, A., Mohr, P.C., Norrman, J., Martin, R.W., Topgaard, D., 2010. Polarization Transfer Solid-State NMR for Studying Surfactant Phase Behavior. Langmuir 26, 16848-16856.

Panchagnula, R., Salve, P.S., Thomas, N.S., Jain, A.K., Ramarao, P., 2001. Transdermal delivery of naloxone: effect of water, propylene glycol, ethanol and their binary combinations on permeation through rat skin. International journal of pharmaceutics 219, 95-105.

Pham, Q.D., Bjorklund, S., Engblom, J., Topgaard, D., Sparr, E., 2016. Chemical penetration enhancers in stratum corneum - Relation between molecular effects and barrier function. Journal of controlled release : official journal of the Controlled Release Society 232, 175-187.

Prausnitz, M.R., Langer, R., 2008. Transdermal drug delivery. Nature biotechnology 26, 1261.

Qi, Q.M., Mitragotri, S., 2019. Mechanistic study of transdermal delivery of macromolecules assisted by ionic liquids. Journal of controlled release : official journal of the Controlled Release Society 311-312, 162-169.

Santos de Almeida, T., Júlio, A., Saraiva, N., Fernandes, A.S., Araújo, M.E.M., Baby, A.R., Rosado, C., Mota, J.P., 2017. Choline- versus imidazole-based ionic liquids as functional ingredients in topical delivery systems: cytotoxicity, solubility, and skin permeation studies. Drug Dev Ind Pharm 43, 1858-1865.

Schwarz, J.C., Pagitsch, E., Valenta, C., 2013. Comparison of ATR–FTIR spectra of porcine vaginal and buccal mucosa with ear skin and penetration analysis of drug and vehicle

components into pig ear. European Journal of Pharmaceutical Sciences 50, 595-600.

Sidat, Z., Marimuthu, T., Kumar, P., du Toit, L.C., Kondiah, P.P.D., Choonara, Y.E., Pillay, V., 2019. Ionic Liquids as Potential and Synergistic Permeation Enhancers for Transdermal Drug Delivery. Pharmaceutics 11.

Sintov, A.C., Zhang, P.J., Michniak-Kohn, B.B., 2009. Cutaneous biotransformation of N-(4-bromobenzoyl)-S,S-dimethyliminosulfurane and its product, 4-bromobenzamide, leading to percutaneous penetration enhancement of drugs: initial evidence using hydrocortisone. Journal of controlled release : official journal of the Controlled Release Society 133, 44-51.

Song, J.F., Lau-Cam, C.A., Kim, K.H., 2001. Monohydroxylation and esterification as determinants of the effects of cis- and trans-9-octadecenoic acids on the permeation of hydrocortisone and 5-fluorouracil across hairless mouse skin in vitro. International journal of pharmaceutics 212, 153-160.

Tanner, E.E.L., Curreri, A.M., Balkaran, J.P.R., Selig-Wober, N.C., Yang, A.B., Kendig, C., Fluhr, M.P., Kim, N., Mitragotri, S., 2019. Design Principles of Ionic Liquids for Transdermal Drug Delivery. Advanced materials 31, e1901103.

Tanner, E.E.L., Ibsen, K.N., Mitragotri, S., 2018. Transdermal insulin delivery using choline-based ionic liquids (CAGE). Journal of controlled release : official journal of the Controlled Release Society 286, 137-144.

Tao, G.-h., He, L., Liu, W.-s., Xu, L., Xiong, W., Wang, T., Kou, Y., 2006. Preparation, characterization and application of amino acid-based green ionic liquids. Green Chemistry 8, 639.

Tao, G.H., He, L., Sun, N., Kou, Y., 2005. New generation ionic liquids: cations derived from

amino acids. Chemical communications, 3562-3564.

Vávrová, K., Hrabálek, A., Doležal, P., Holas, T., Zbytovská, J., 2003a. l-Serine and glycine based ceramide analogues as transdermal permeation enhancers: polar head size and hydrogen bonding. Bioorganic & medicinal chemistry letters 13, 2351-2353.

Vávrová, K., Hrabálek, A., Doležal, P., Šámalová, L., Palát, K., Zbytovská, J., Holas, T., Klimentová, J., 2003b. Synthetic ceramide analogues as skin permeation enhancers: structure–Activity relationships. Bioorganic & Medicinal Chemistry 11, 5381-5390.

Venuganti, V.V.K., Perumal, O.P., 2008. Effect of poly(amidoamine) (PAMAM) dendrimer on skin permeation of 5-fluorouracil. International journal of pharmaceutics 361, 230-238.

Wang, C., Zhu, J., Zhang, D., Yang, Y., Zheng, L., Qu, Y., Yang, X., Cui, X., 2018. Ionic liquid - microemulsions assisting in the transdermal delivery of Dencichine: Preparation, in-vitro and in-vivo evaluations, and investigation of the permeation mechanism. International journal of pharmaceutics 535, 120-131.

Wang, M., Xi, H., Cun, D., Chen, Y., Xu, Y., Fang, L., 2013. l-Carvyl esters as penetration enhancers for the transdermal delivery of 5-fluorouracil. AAPS PharmSciTech 14, 669-674.

Wertz, P.W., 1996. The nature of the epidermal barrier: biochemical aspects. Advanced drug delivery reviews 18, 283-294.

Wu, X., Chen, Z., Li, Y., Yu, Q., Lu, Y., Zhu, Q., Li, Y., An, D., Qi, J., Wu, W., 2019. Improving dermal delivery of hydrophilic macromolecules by biocompatible ionic liquid based on choline and malic acid. International journal of pharmaceutics 558, 380-387.

Xie, W.J., Zhang, Y.P., Xu, J., Sun, X.B., Yang, F.F., 2017. The Effect and Mechanism of Transdermal Penetration Enhancement of Fu's Cupping Therapy: New Physical Penetration

Technology for Transdermal Administration with Traditional Chinese Medicine (TCM) Characteristics. Molecules 22.

Yang, S., Wang, R., Wan, G., Wu, Z., Guo, S., Dai, X., Shi, X., Qiao, Y., 2016. A Multiscale Study on the Penetration Enhancement Mechanism of Menthol to Osthole. J Chem Inf Model 56, 2234-2242.

Zakrewsky, M., Lovejoy, K.S., Kern, T.L., Miller, T.E., Le, V., Nagy, A., Goumas, A.M., Iyer, R.S., Del Sesto, R.E., Koppisch, A.T., Fox, D.T., Mitragotri, S., 2014. Ionic liquids as a class of materials for transdermal delivery and pathogen neutralization. Proceedings of the National Academy of Sciences 111, 13313-13318.

Zhang, D., Wang, H.-J., Cui, X.-M., Wang, C.-X., 2017. Evaluations of imidazolium ionic liquids as novel skin permeation enhancers for drug transdermal delivery. Pharmaceutical development and technology 22, 511-520.

Zhang, S., Sun, N., He, X., Lu, X., Zhang, X., 2006. Physical Properties of Ionic Liquids: Database and Evaluation. Journal of Physical and Chemical Reference Data 35, 1475.

Zhao, L., Fang, L., Xu, Y., Liu, S., He, Z., Zhao, Y., 2008. Transdermal delivery of penetrants with differing lipophilicities using O-acylmenthol derivatives as penetration enhancers. European journal of pharmaceutics and biopharmaceutics : official journal of Arbeitsgemeinschaft fur Pharmazeutische Verfahrenstechnik e.V 69, 199-213.

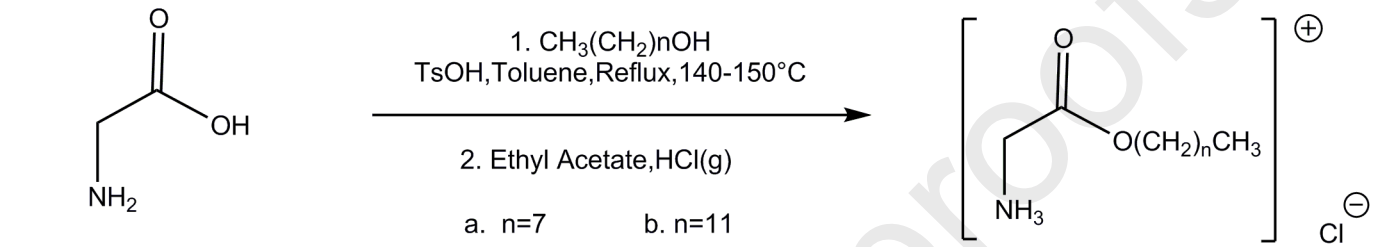

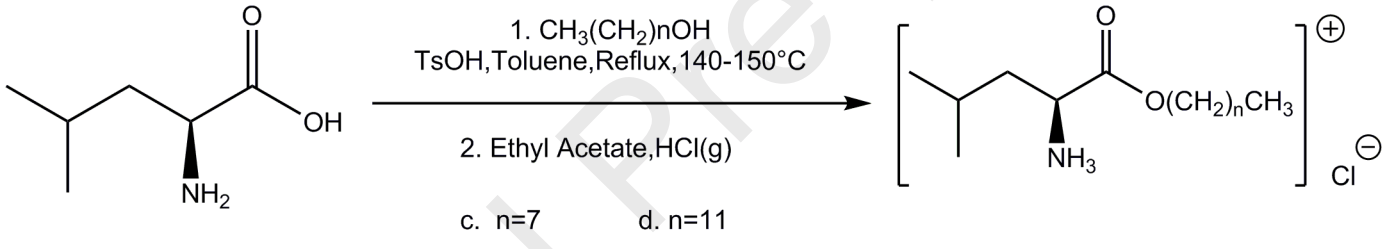

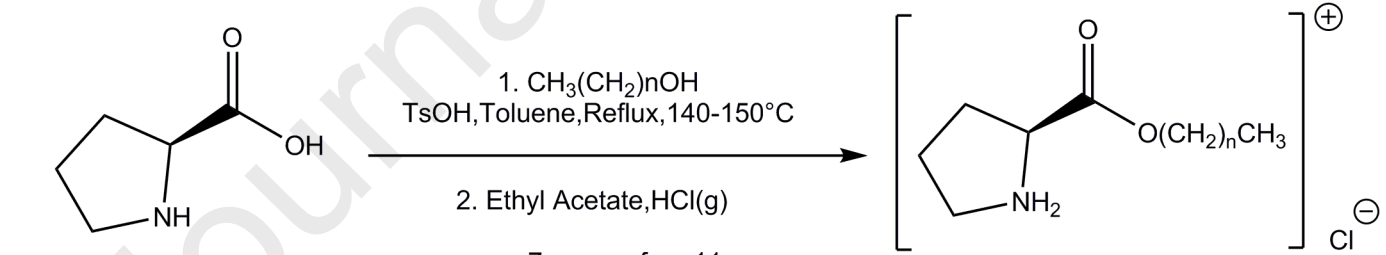

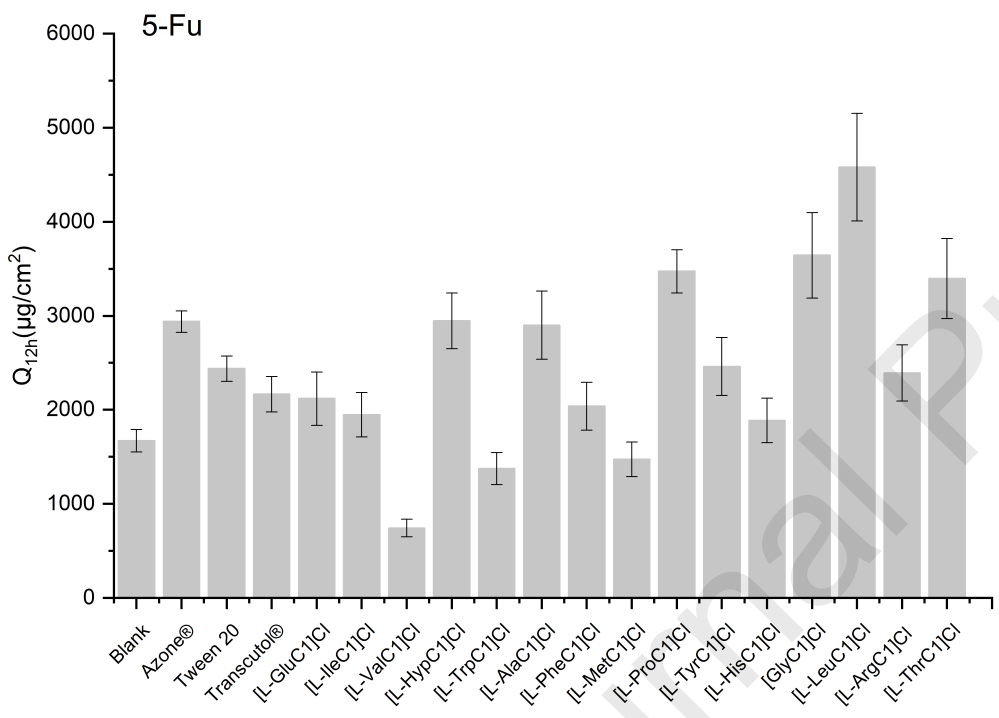

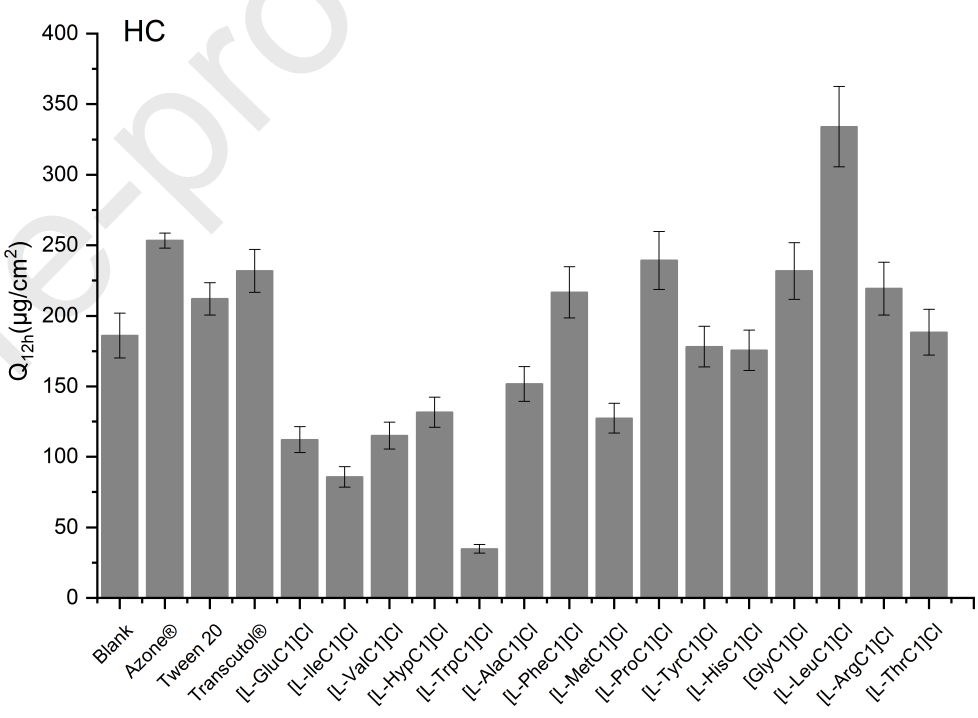

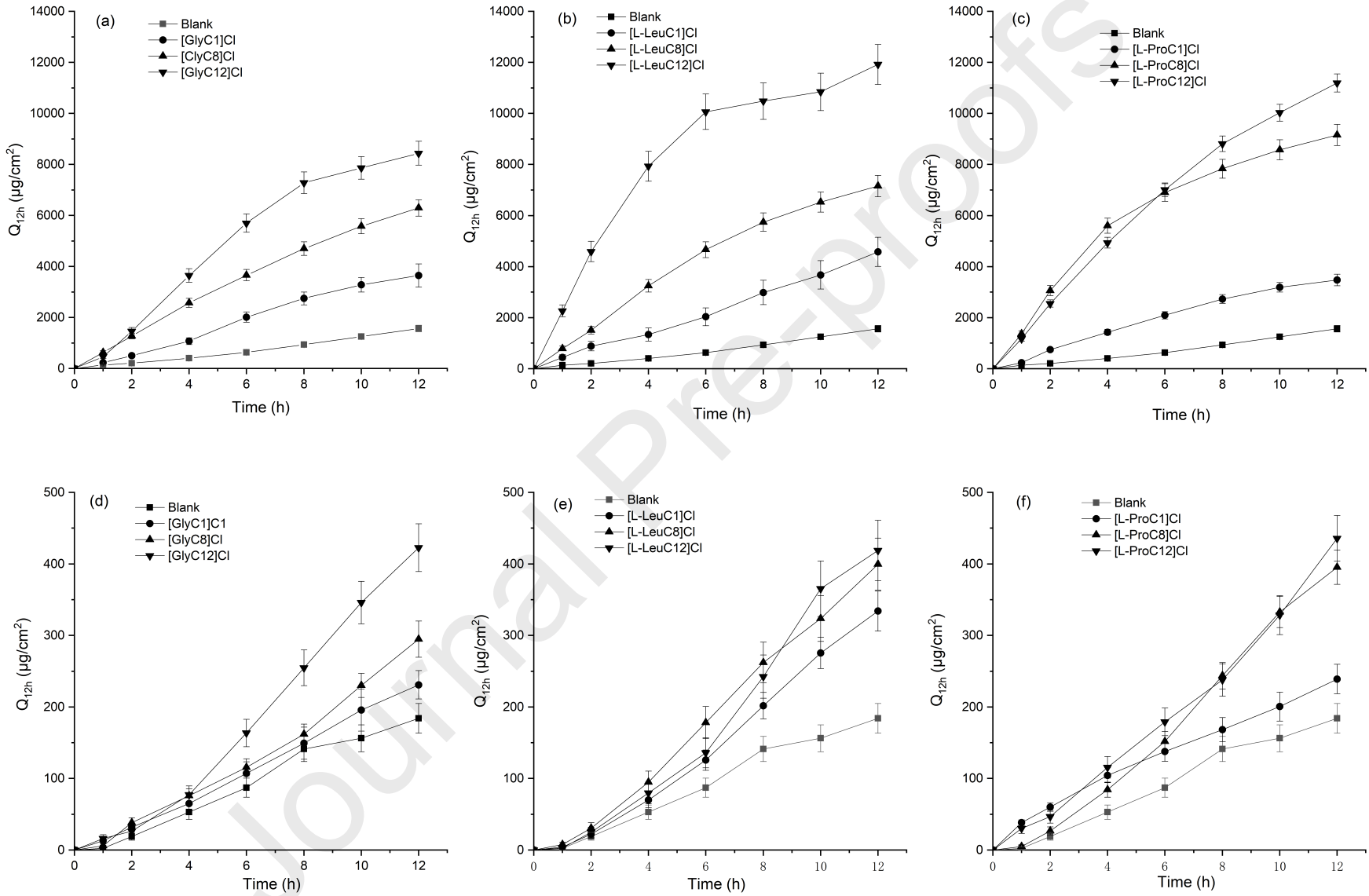

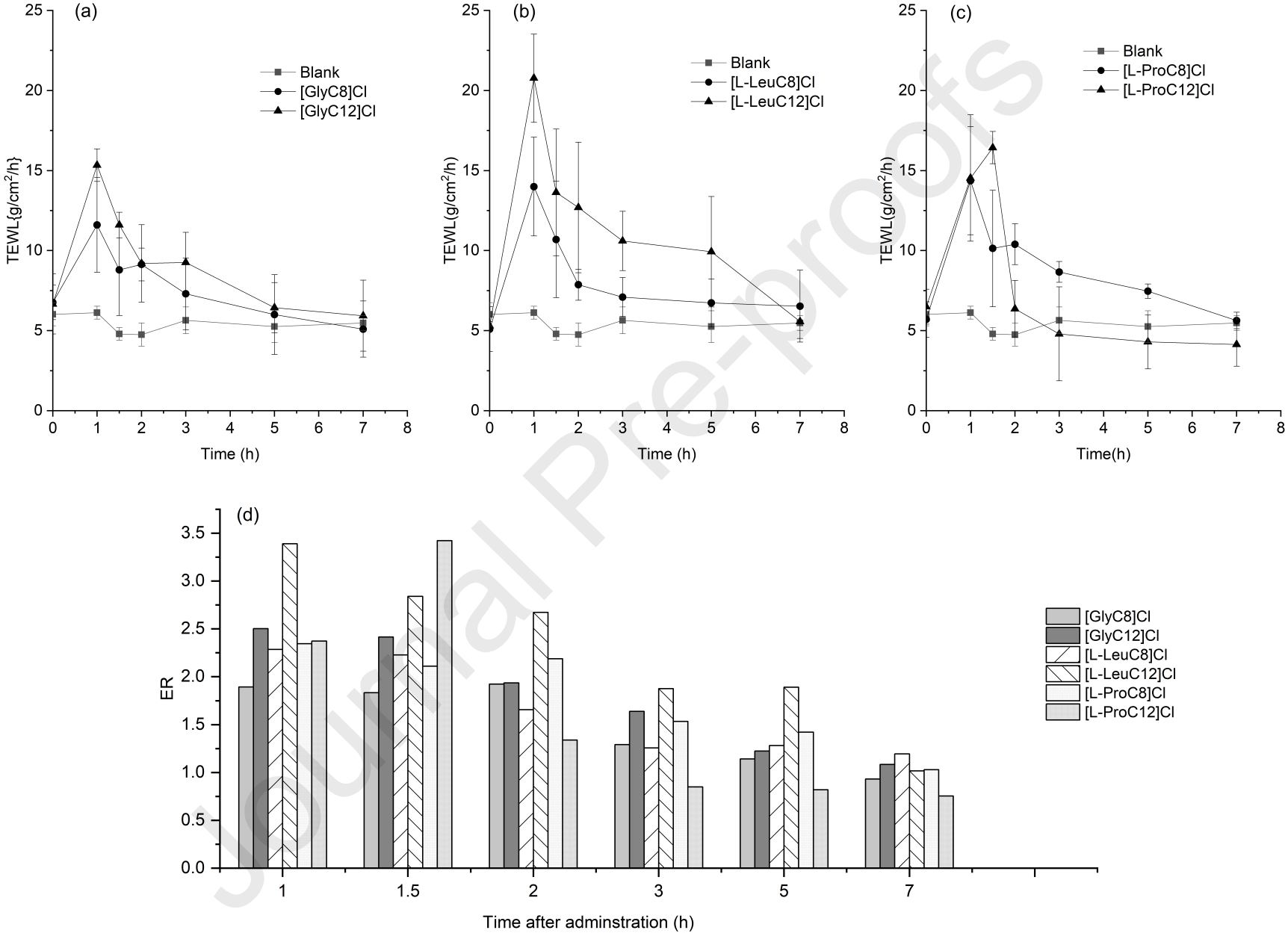

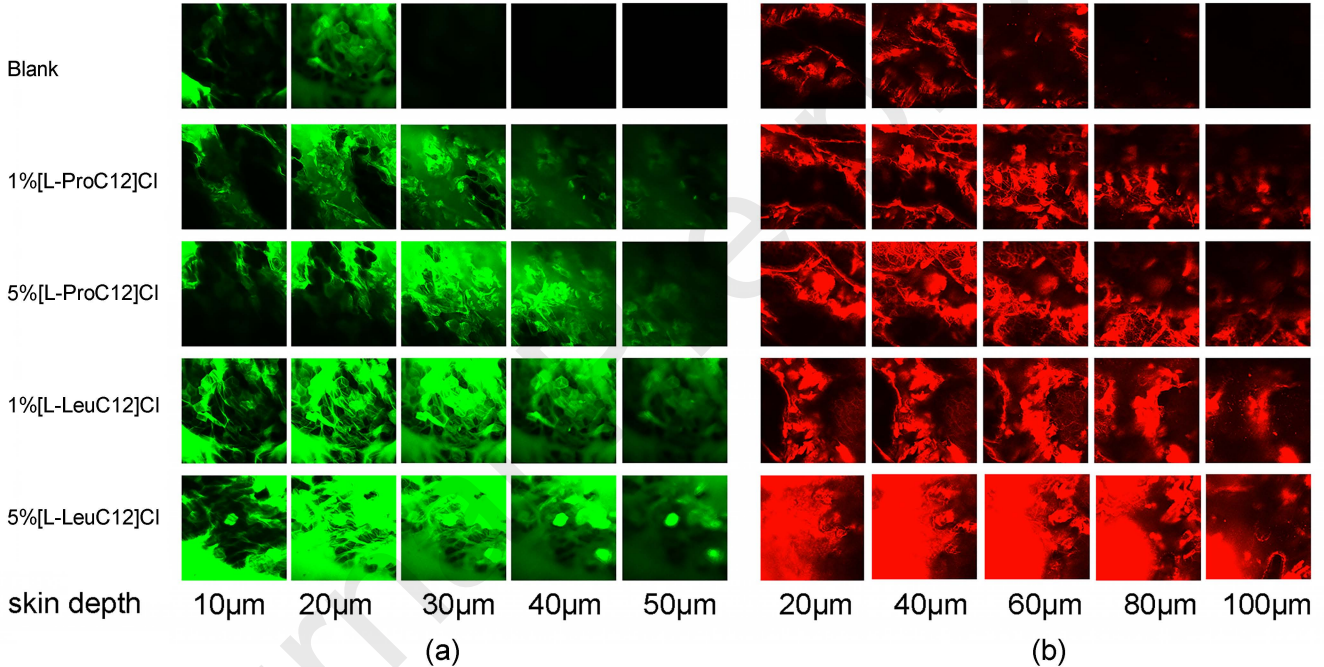
Blank
1%[L-ProC12]Cl
5%[L-ProC12]Cl
1%[L-LeuC12]Cl
5%[L-LeuC12]Cl
skin depth
10μm
20μm
30μm
40μm
50μm
(a)
20μm
40μm
60μm
80μm
100μm
(b)

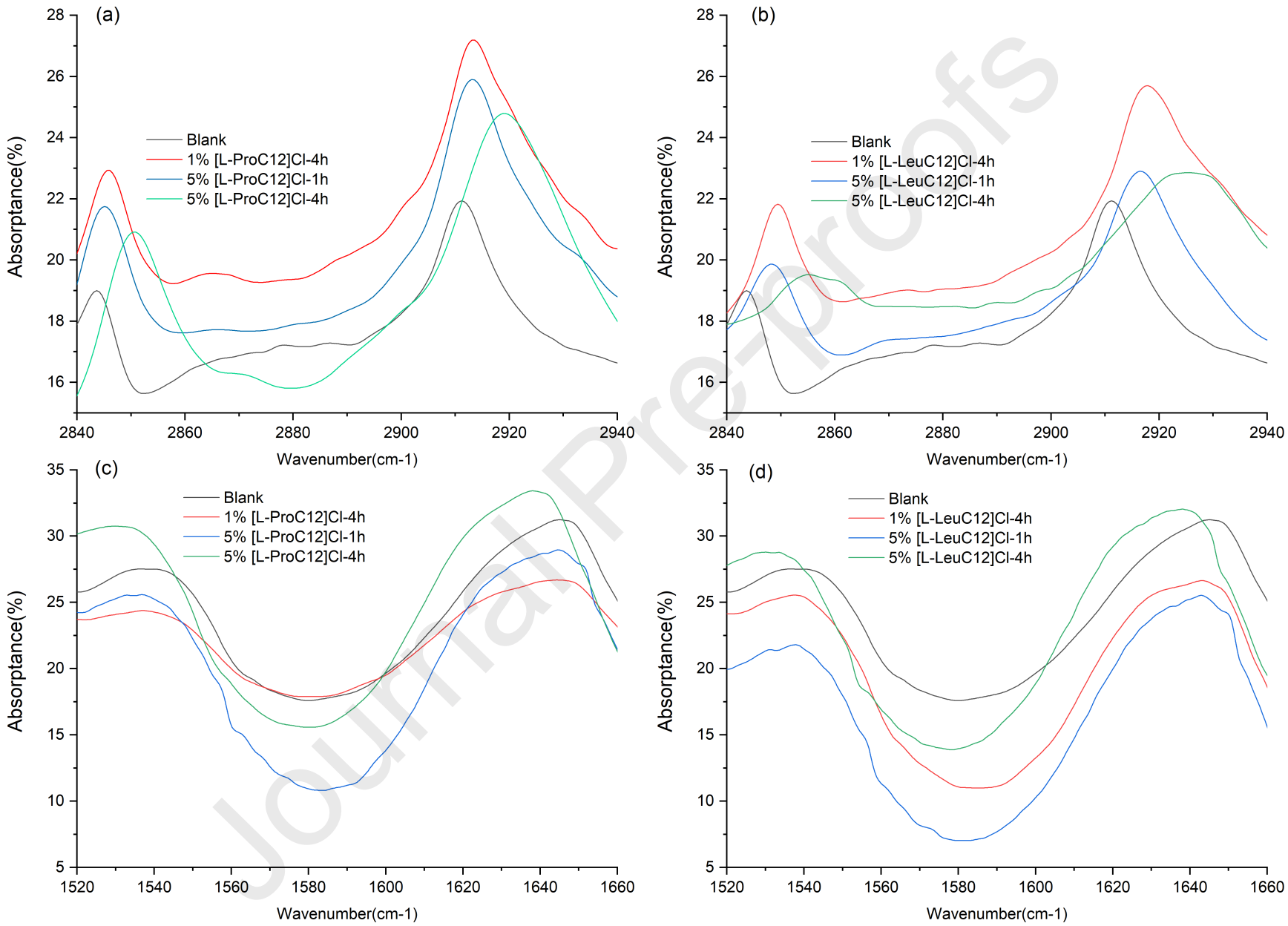

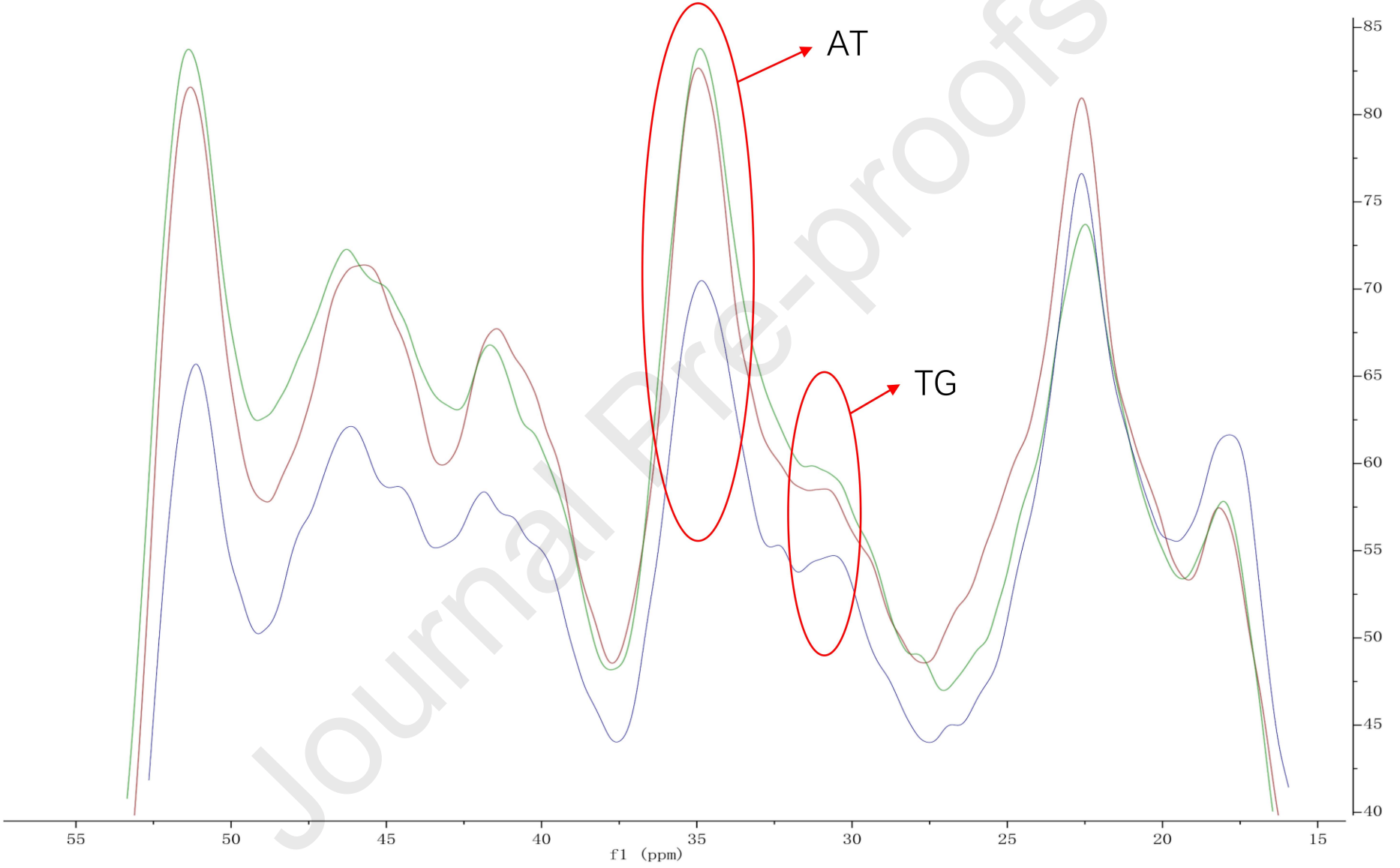

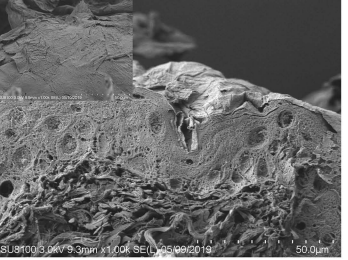

(a) Blank

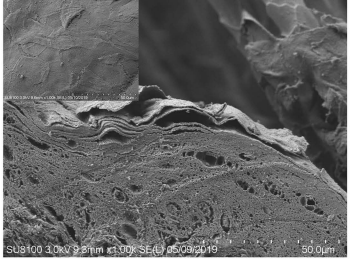

(b) 1 % [L-ProC12]Cl 4h

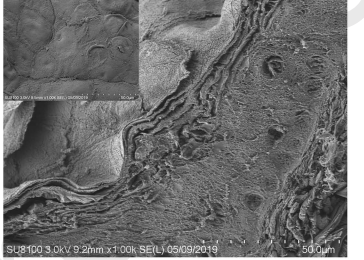

(c) 5%[L-ProC12]Cl 1h

(d) 5%[L-ProC12]Cl 4h

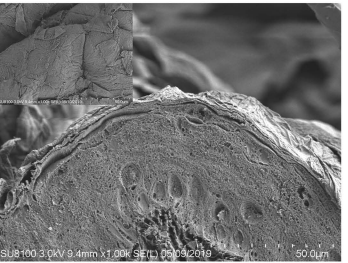

(e) Normal Saline

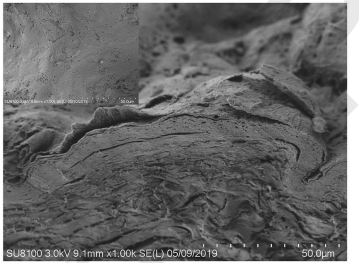

(f) 1% [L-LeuC12]Cl 4h

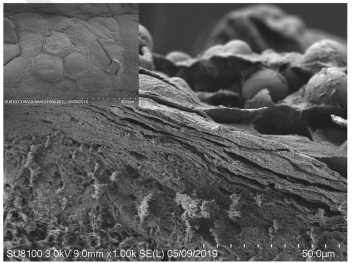

(g) 5%[L-LeuC12]Cl 1h

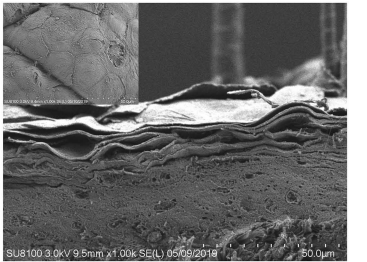

(h) 5%[L-LeuC12]Cl 4h

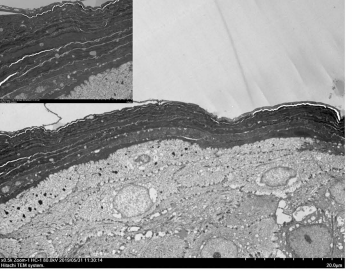

(a) Blank

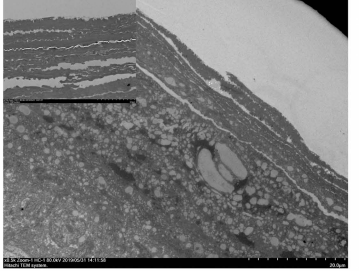

(b) 1% [L-ProC12]Cl 4h

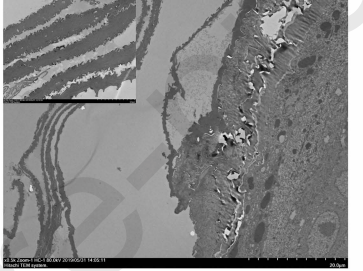

(c) 5% [L-ProC12]Cl 1h

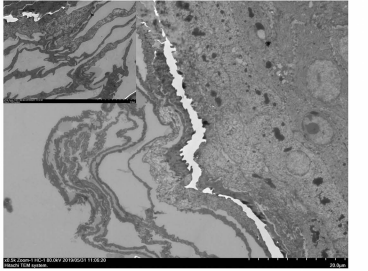

(d) 5%[L-ProC12]Cl 4h

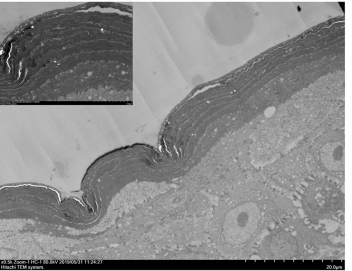

(e) Normal saline

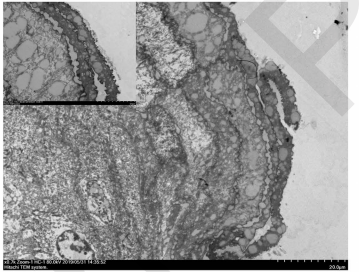

(f) 1% [L-LeuC12]Cl 4h

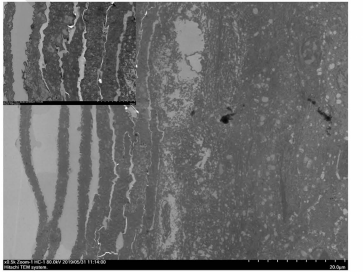

(g) 5% [L-LeuC12]Cl 1h

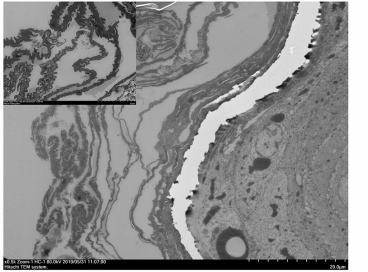

(h) 5%[L-LeuC12]Cl 4h

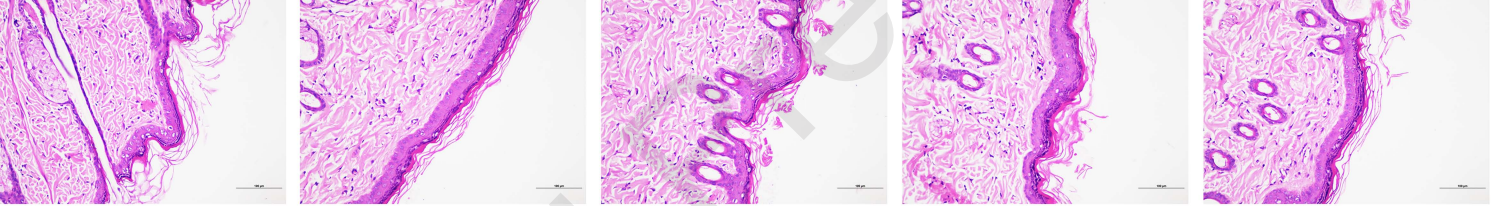

Blank 5%[L-ProC12]Cl 1h 5%[L-ProC12]Cl 4h 5%[L-LeuC12]Cl 1h 5%[L-LeuC12]Cl 4h

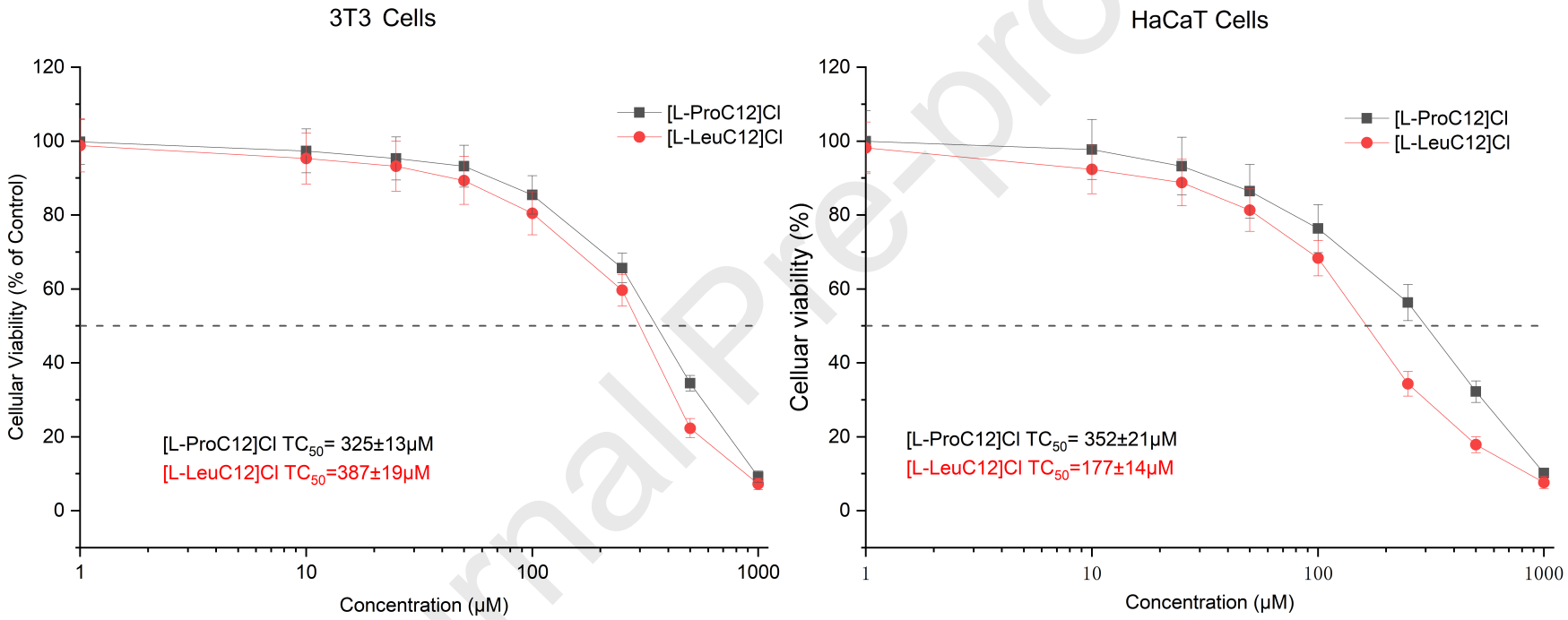
3T3 Cells
HaCaT Cells
[L-ProC12]Cl
[L-LeuC12]Cl
Cellular Viability (% of Control)
Celluar viability (%)
Concentration (μM)
[L-ProC12]Cl TC50= 325±13μM
[L-LeuC12]Cl TC50=387±19μM
[L-ProC12]Cl TC50= 352±21μM
[L-LeuC12]Cl TC50=177±14μM

Table 1 Skin permeation parameters of HC and 5-Fu under the treatment of the 15 [AAE] ILs (mean±S.D, n=4).

	5-Fu			HC		
	Flux ($\mu g/cm^2/h$)	Pm (cm/h)	ER	Flux (μg/cm2/h)	Pm (cm/h)	ER
Blank	140.35 ±7.40	2.81±0.15	1.00	15.70 ±1.39	1.45 ±0.13	1.00
Azone®	236.11±5.32	4.82±0.11	1.73	22.54± 1.55	2.03±0.09	1.39
Tween20	203.12±6.98	3.99±0.16	1.41	18.80±1.71	1.70±0.11	1.12
Transcutol®	185.33±11.22	3.79±0.15	1.32	20.33 ±1.33	1.83±0.12	1.23
[L-GluC1]Cl	175.21 ±9.37	3.50±0.19	1.27	9.32 ±0.21	0.86±0.02	0.60
[L-IleC1]Cl	160.76 ±10.17	3.22±0.20	1.17	7.24 ±0.60	0.67±0.06	0.46
[L-ValC1]Cl	62.11 ±1.15	1.24±0.02	0.45	9.60±0.11	0.89±0.01	0.62
[L-hypC1]Cl	246.89±8.42	4.94±0.17	1.76	10.79±1.29	1.00 ±0.12	0.71
[L-TrpC1]Cl	114.71±1.17	2.29±0.02	0.82	2.98 ±0.45	0.28±0.04	0.19
[L-AlaC1]Cl	245.07±22.45	4.90±0.45	1.74	12.45±1.38	1.15±0.13	0.82
[L-PheC1]Cl	168.03±12.46	3.36±0.25	1.22	18.13±0.48	1.68±0.04	1.17
[L-MetC1]Cl	121.51 ±8.61	2.43±0.17	0.88	10.54±0.49	0.98±0.05	0.68
[L-ProC1]Cl	291.53±13.57	5.83±0.27	2.08	20.27±2.17	1.87±0.20	1.29
[L-TyrC1]Cl	203.47±11.10	4.07±0.22	1.47	14.64±1.50	1.35±0.14	0.96
[L-HisC1]Cl	156.20±6.75	3.12±0.14	1.13	14.48±1.11	1.34±0.10	0.94
[L-GlyC1]Cl	302.57±7.00	6.05±0.14	2.18	19.79±3.13	1.83±0.29	1.25
[L-leuC1]Cl	383.16±9.20	7.66±0.18	2.74	22.96±2.44	2.10±0.23	1.80
[L-ArgC1]Cl	201.0811.15±	4.02±0.22	1.43	18.53±1.70	1.71±0.16	1.18
[L-ThrC1]Cl	284.09±6.56	5.68±0.13	2.03	16.00 ±2.02	1.48±0.19	1.01

Table 2 Skin permeation parameters of HC and 5-Fu under the treatment of the six modified [AAE] ILs (mean±S.D, n=4).

	5-Fu			HC		
	Flux (μg/cm^2/h)	P_m×10^2 (cm/h)	ER	Flux (μg/cm^2/h)	P_m×10^2 (cm/h)	ER
Blank	140.35 ±7.40	2.81±0.15	1.00	15.70 ±1.39	1.45 ±0.13	1.00
[GlyC1]Cl	302.57±44.00[a]	6.05±0.14[a]	2.18	19.79±3.13[d]	1.83±0.29 [d]	1.25
[GlyC8]Cl	449.44±63.64[a,b]	8.99±1.27 [a,b]	3.77	21.05±3.49[d]	1.92±0.32 [d]	1.60
[GlyC12]Cl	602.55±68.90 [a,b,c]	12.05±1.69 [a,b,c]	5.05	30.19±5.27[a,,e]	2.76 ±0.64 [a,,e]	2.30
[L-LeuC1]Cl	383.16±29.20[a]	7.66±0.18	2.74	22.96±2.44[d]	2.10±0.23 [a]	1.80
[L-LeuC8]Cl	511.11±52.03 [a,b]	10.22±0.97 [a,b]	4.28	28.54±4.31[a,e]	2.61±0.41 [a]	2.17
[L-LeuC12]Cl	851.47±69.49 [a,b,c]	17.03±1.45 [a,b,c]	7.14	29.92±5.33[a,e]	2.73 ±0.44 [a,]	2.28
[L-ProC1]Cl	291.53±13.57[a]	5.83±0.27[a]	2.08	20.27±2.17[d]	1.87±0.20 [d]	1.29
[L-ProC8]Cl	654.20 ±66.56 [a,b]	13.08±1.01 [a,b]	5.48	28.24±4.78[a,e]	2.58±0.41 [a,e]	2.15
[L-ProC12]Cl	672.71 ±68.78 [a,b]	13.45±1.49 [a,b]	5.64	31.12±4.29[a,e]	2.90±0.35 [a,e]	2.37

a: comparing with blank, p<0.01; b: comparing with the [AAC1]Cl, p<0.01;c: comparing with the [AAC8]Cl, p<0.05; d: a: comparing with blank, p<0.05;e: comparing with the [AAC1]Cl,p<0.05

Table 3 Characteristic ATR-FTIR absorptions of the mice skin under the treatment of the six modified [AAE] ILs (mean±S.D, n=4).

Group	Control	[L-ProC12]Cl			[L-LeuC12]Cl		
		1%-4h	5%-1h	5%-4h	1%-4h	5%-1h	5%-4h
=-OH	3273.96±4.52	3269.51±2.14	3273.56±2.65	3273.81±1.77	3271.34±1.04	3271.35±2.10	3271.65±2.34
VasCH$_2$	2915.52±2.90	2917.25±1.32	2917.05±2.31	2921.32±1.37*	2919.88±2.50	2918.66±0.71*	2922.01±0.27**
VsCH$_2$	2846.27±1.49	2847.09±1.23	2847.15±0.64	2852.21±0.28*	2850.80±1.62	2850.41±1.04*	2853.48±0.16**
C=O	1738.60±1.94	1734.49±1.39	-	1734.60±4.37	1741.22±3.91	1735.39±3.41	1738.44±2.06
NH-C=O	1645.42±1.54	1643.10±1.93	1643.12±1.66	1641.60±0.67*	1644.12±0.66	1644.56±1.27	1641.60±1.66*
NH-C=O	1542.50±1.86	1540.19±2.76	1539.54±1.32*	1536.69±1.59*	1541.24±0.62	1540.69±2.43*	1537.61±2.06*

*: $p<0.05$, compared with control; **:$p<0.01$, compared with control.

Graphical abstract

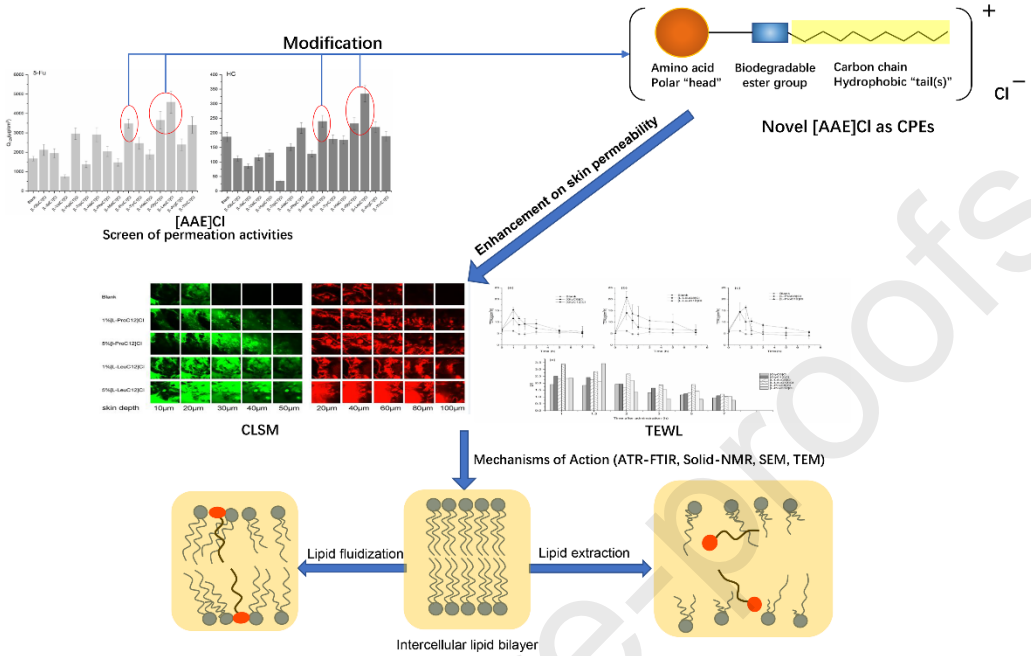

Declarations of interest

All the authors declare that there are no conflicts of interest.

Chengxiao Wang contributed to the conception of the work and wrote the manuscript.

Yaming Li contributed significantly to the synthesis methods of AAE-ILs.

Luyao Zheng and Zhiyuan Zhao performed the whole experiment and analyzed the data.

Ye Yang helped perform the analysis with constructive discussions.